Rev. Adv. Mater. Sci. 47 (2016) 79-85

SUPERPLASTICITY OF HIGHLY DISCLINATED GRAPHENE

A.S. Kochnev[1,2], I. A. Ovid'ko[1,2,3] and B. N. Semenov[1,2,3]

[1]Peter the Great St. Petersburg Polytechnic University, St. Petersburg 195251, Russia
[2]St. Petersburg State University, St. Petersburg 199034, Russia
[3]Institute of Problems of Mechanical Engineering, Russian Academy of Sciences, St. Petersburg 199178, Russia

Received: November 10, 2016

Abstract. Deformation and fracture processes in highly disclinated graphene – graphene containing a high-density ensemble of rectangular disclination quadrupoles - are examined by molecular dynamics simulations. A special disclination mechanism of plastic deformation in graphene is discussed. Also, we consider the effects of disclination-induced curvature in graphene on its mechanical characteristics, namely stress-strain dependence, elastic limit, strain-to-failure and tensile strength. In particular, our simulations reveal that the highly disclinated graphene exhibits superplasticity specified by strain-to-failure ≈ 234%. The key reason of superplasticity is in the presence of pre-existent disclinations that enhance generation of new disclination dipoles and other disclination configurations carrying plastic flow in graphene.

1. INTRODUCTION

Graphene – a carbon monolayer with the covalently bonded hexagonal crystal structure – shows the unique electronic, energy-storage, thermal and mechanical properties being of tremendous interest for a wide range of technologies; see, e.g., reviews [1-10]. For instance, following the experimental data [11], pristine graphene is specified by such outstanding mechanical characteristics as superior intrinsic strength of ≈ 130 GPa, superior elastic strain of 25% and extraordinarily high Young modulus of ≈ 1.0 TPa. These characteristics are crucially important for structural applications of graphene and its exploitation in nanoelectronics where its mechanical properties are critical for lifetime of graphene-based devices.

Also, graphene demonstrates the excellent electronic properties due to its 2D hexagonal crystal structure and the presence of charge carriers that behave like massless particles [1,4,6]. One of the most effective approaches to modify, design and control the remarkable electronic properties of graphene is based on their sensitivity to local curvature and associated elastic strains in graphene; see, e.g., [12-17]. For instance, the pronounced sensitivity of the electronic properties exhibited by graphene to curvature-produced strains in its structure distinctly manifests itself in the giant strain-induced pseudo-magnetic field in graphene nanobubbles [14]. The experiment [14] under discussion is a good example of tuning and controlling the electronic properties of graphene through its curvature engineering.

At the same time, research efforts addressing the effects of curvature on the mechanical properties of graphene are very limited [19-21]. In particular, in paper [19], graphene with a high-density ensemble of homogeneously dispersed topological disclinations was defined and theoretically described as a new two-dimensional material called highly disclinated graphene (HDG). Following [19], 5- and 7-disclinations – pentagon and heptagon rings of carbon atoms – in hexagonal lattice of graphene

Corresponding author: I.A. Ovidko, e-mail: ovidko@nano.ipme.ru

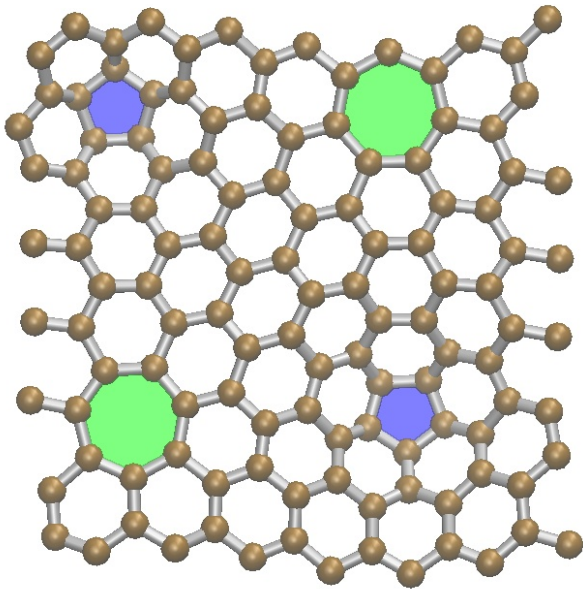

Fig. 1. Simulation cell of highly disclinated graphene contains a quadrupole of 5- and 7-disclinations (pentagon and heptagon rings of carbon atoms, respectively) in hexagonal lattice of graphene. 5- and 7-disclinations are colored by blue and green, respectively.

create the nanoscopically buckled structure containing local "hills" and "valleys". It is theoretically predicted that the buckled structure may cause potentially excellent mechanical characteristics of HDG. The main aim of this paper is to examine by molecular dynamics (MD) simulations both deformation and fracture processes in HDG with a special attention being devoted to the curvature effects in HDG on its mechanical characteristics, such as stress-strain dependence, elastic limit, strain-to-failure and tensile strength. In particular, our simulations reveal a very intriguing and practically important feature of the deformation behavior exhibited by HDG, namely its superplasticity specified by strain-to-failure $\approx$ 234%.

2. SIMULATION METHODS

In description of deformation and fracture processes in HDG, we used the Large-scale Atomic/Molecular Massively Parallel Simulator MD simulation package. In order to specify interatomic bonds, the adaptive intermolecular reactive bond order (AIREBO) potential [22] is utilized which is conventionally exploited in computer models of deformation and fracture processes in graphene materials; see, e.g., [21,23-29].

The 3D simulation cell contains 120 carbon atoms and is specified by periodic boundary conditions along vertical and horizon directions in Fig. 1. At the first stage of the pre-simulation procedure, we create a flat HDR specimen containing a regular lattice of rectangular quadrupoles of 5- and 7-disclinations in the hexagonal lattice of graphene (Fig. 1). Disclinations belonging to a quadrupole in HDG generate high in-plane stresses localized in the vicinity of the quadrupole. (Disclination quadrupoles do not generate long-range stresses, because stress fields of 5- and 7-disclinations belonging to one quadrupole are mutually screened [19], as with discination quadrupoles in 3D solids [30,31].) In these circumstances, HDG in its flat state contains highly distorted hexagon cells of carbon atoms (Fig. 1). The 3D simulation cell of HDG in its initial (pre-deformation) flat state has the length of 17.7 Å and width of 17.5 Å. The distance between carbon atoms in graphene in its initial state is taken as 1.42 Å.

At the second stage of the pre-simulation procedure, the initial flat HDG model was relaxed through simulations involving 1,000,000 iteration steps in Nose-Hoover thermostat at room temperature (300K). As a result of the relaxation procedure, the initially flat GNR is transformed into a nanoscopically buckled structure containing local "hills" and "valleys" associated with 5- and 7-disclinations, respectively (Fig. 2). The reason for generation of curvature in the HDG (Fig. 2) is related to balance between elastic energies that specify flat and curved configurations of graphene containing disclinations [19]. In short, in the absence of external mechanical load, the elastic energy of HDG in its curved configuration (Fig. 2) is much lower than that in its flat counterpart. With this factor, the HDG tends to be curved (Fig. 2) when external mechanical load is absent.

Then the tensile strain was applied with a strain rate of 0.0005 per femtosecond. The tension is applied along the horizontal direction in plane shown in Fig. 1. Evolution of the HDG structure under tensile deformation will be considered in detail in next section. In doing so, illustrative figures will be presented showing projection of the HSD structure onto plane where its initial flat state was pre-simulated (Fig. 1).

3. DEFECTS, DEFORMATION AND FRACTURE PROCESSES IN HIGHLY DEFECTED GRAPHENE

The HDG (Fig. 2) represents a good example of graphene nanostructures in which the curvature effects on mechanical properties of graphene

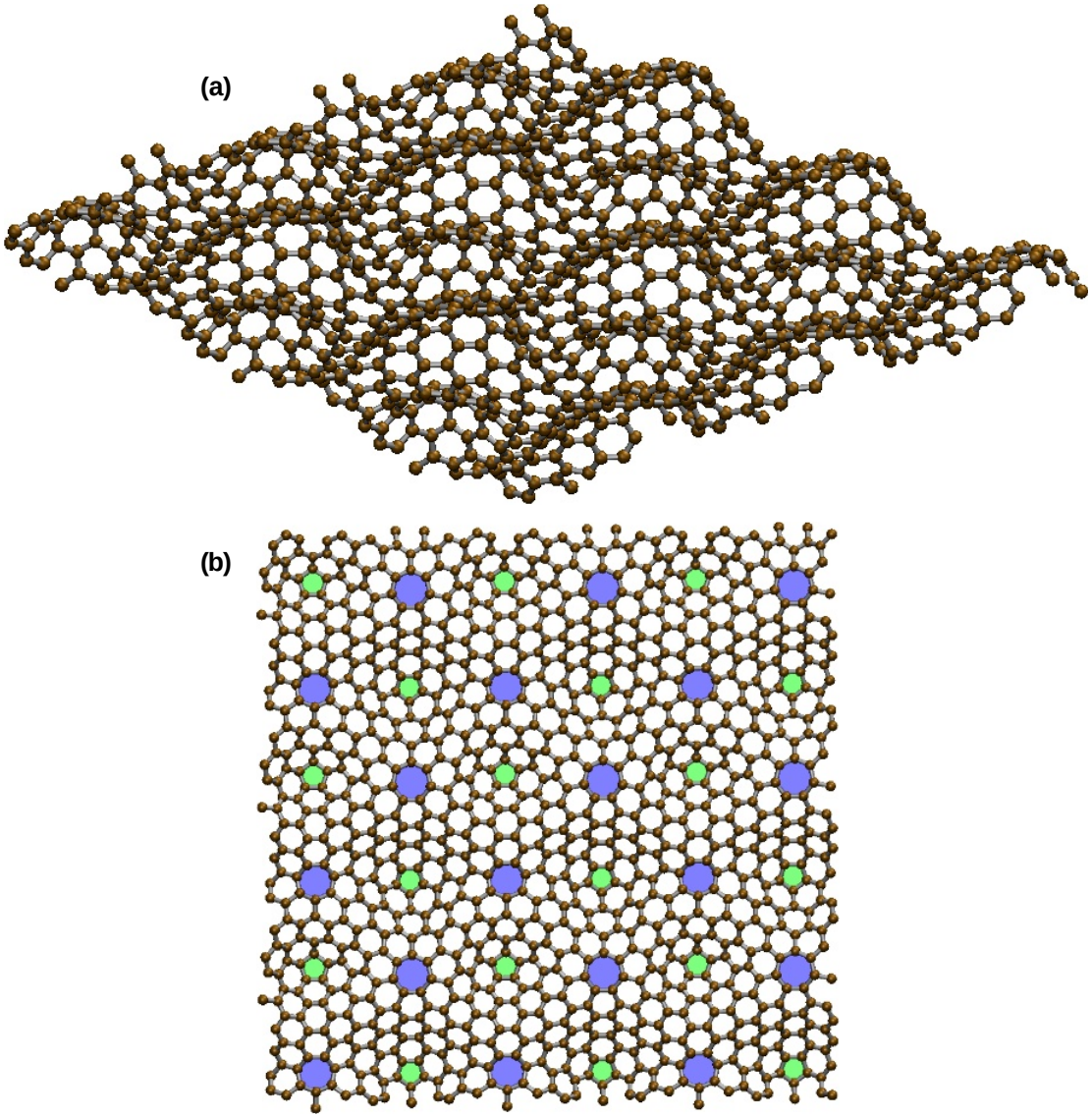

Fig. 2. Highly disclinated graphene represents a graphene monolayer containing a high-density ensemble of rectangular disclination quadrupoles after relaxation. (a) General 3D view. The relaxed structure of highly disclinated graphene contains local “hills” and “valleys” associated with 5- and 7-disclinations, respectively. (b) 2D projection of the relaxed structure of highly disclinated graphene.

effectively come into play. In order to identify and describe such effects, we simulate tensile test of buckled HDG. Our MD simulations show that the curved HDG is, in part, flattened under tension load. In this case, the bending energy accumulated in HDG is, in part, transformed into the stretching energy, and in-plane stresses of the disclinations become pronounced. Also, the mechanical load induces generation of new 5- and 7-disclinations as well as crack-like *n*-cells, that is, *n*-membered rings of carbon atoms, where $n > 7$ (Fig.3.). More precisely, HDG shown in Fig. 3 contains crack-like n-cells specified by $n = 8$, 11, and 13. Crack-like cells are generated through breaks of interatomic C-C bonds which are typically located at 5- or 7-disclinations or other crack-like cells (because orientations of such bonds deviate from those of the strongest C-C bonds characterizing regular, 6-membered rings of carbon atoms in graphene). For instance, each of crack-like 11-cells (Fig. 3) is generated through break of the C-C bond belonging to neighbouring 5- and 7-disclinations or, in other words, through convergence of these disclinations. Crack-like 13-cell (Fig. 3) is generated through break of the C-C bond belonging to two neighbouring 7-disclinations or, in other words, through convergence of these disclinations.

Further elongation of HDG under tension load is accompanied by generation of new n-disclinations and their convergence (that gives rise to an increase

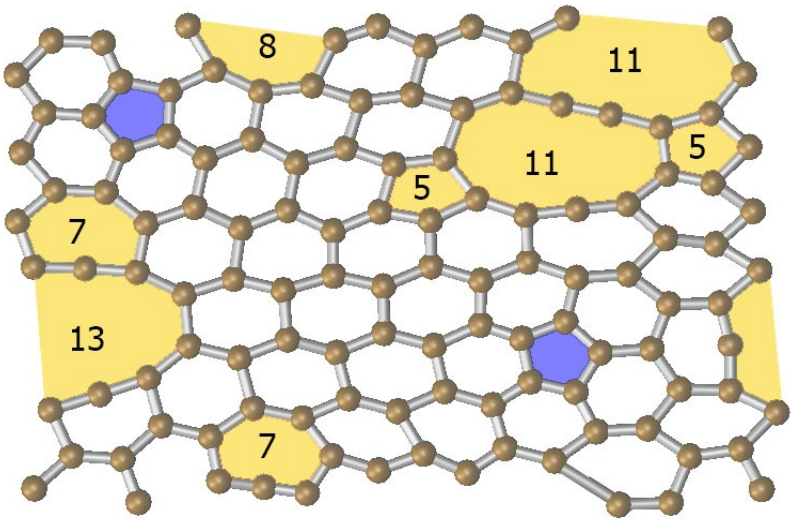

Fig. 3. Deformed cell of highly disclinated graphene at strain $\varepsilon = 55\%$. New *n*-disclinations (that are different from initial ones) are coloured yellow and specified by their non-six numbers *n*.

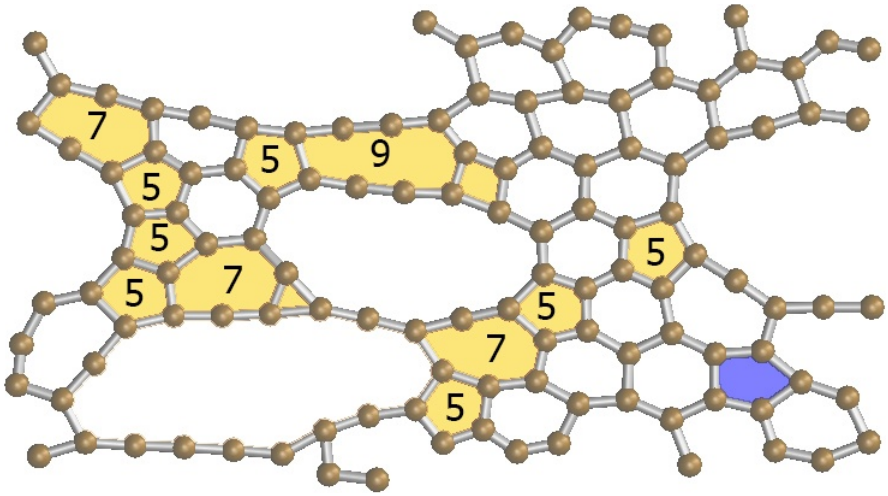

Fig. 4. Deformed cell of highly disclinated graphene at strain $\varepsilon = 85\%$. The cell contains very large pores.

in an average value of *n*) in HDG (Fig. 4). These processes result in the formation of nanoscale cracks/pores that separate HDG into two pieces joined by a monatomic carbon chain (Fig. 5). With further elongation, a break of the monatomic carbon chain occurs (Fig. 6) which realizes complete failure, that is, complete separation of HDG into two separate pieces.

Let us discuss the roles of n-disclinations in plastic deformation and fracture processes occurring in HDG. First, note that point n-disclinations in 2D graphene serve as analogues of line disclinations in conventional 3D materials where dipoles of these line disclinations effectively carry plastic flow; see, e.g., [31-35]. In particular, dipoles and other configurations of line disclinations can significantly contribute to plastic deformation of nanocrystalline 3D materials [31-35]. In the context discussed, it is logical to think that dipoles and other configurations of *n*-disclinations are capable of carrying plastic deformation in graphene. This statement is well consistent with both the experimental observation of plastic deformation carried by dislocations (disclination dipoles) in graphene [32] and the computer simulations demonstrating that *n*-disclinations are intensively generated during plastic deformation of graphene [21,40,41].

Let us consider the situation where no atoms are removed from a mechanically loaded graphene specimen and no new atoms are added to such a specimen. In the situation under consideration, one can distinguish the two basic processes related to transformations of interatomic (C-C) bonds, evolution of *n*-disclinations, and associated deformation and fracture events in graphene. These processes are re-arrangements (flip events) and irreversible debondings (break events) of C-C bonds.

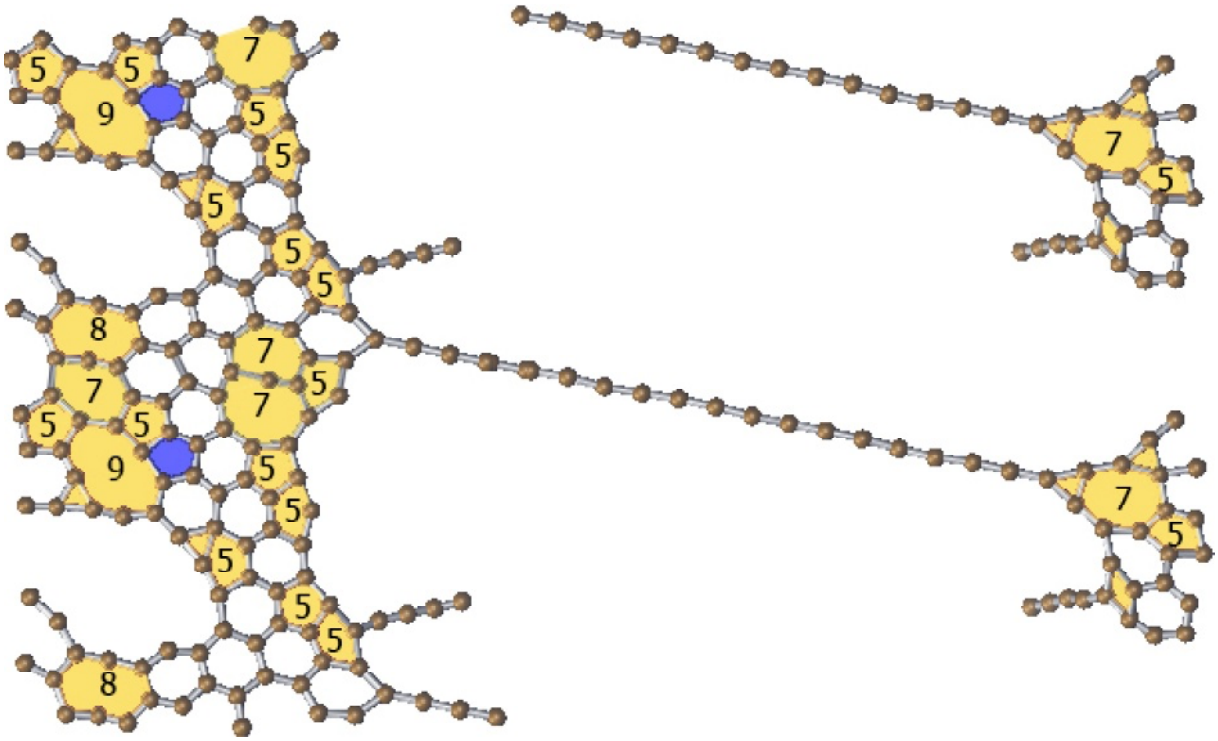

Fig. 5. Deformed cells of highly disclinated graphene at strain ε = 224%. (For clarity, two simulation cells are shown.) Deformation gives rise to separation of each graphene cell into two pieces joined by a monatomic carbon chain.

Fig. 6. Complete fracture occurs at ε = 234%.

Flip events are recognized as elementary events of plastic deformation in carbon nanotubes [36] and graphene [37]. For instance, flip events (rotations of C-C bonds) in hexagonal crystal lattices of graphene and carbon nanotubes create Stone-Wales defects (quadrupoles of neighbouring 5- and 7-disclinations) and provide slip of dislocations (dipoles of 5- and 7-disclinations) [36,37], that is, in our terms, plastic flow through motion of disclination dipoles.

Irreversible break events destroy interatomic C-C bonds and do not create new C-C bonds in mechanically loaded graphene. In the context discussed, irreversible break events are treated as elementary events of fracture/pre-fracture processes in graphene.

4. STRESS-STRAIN DEPENDENCE

Also, with the MD simulations, we revealed stress-strain dependence (Fig. 7), fracture strain and tensile strength that characterize HDG. The stress-strain curve (Fig. 7) has the elastic stage when the strain ε ranges from 0% to the elastic limit $\varepsilon_{el} \approx 40$ % (Fig. 7). It is a rather high value; it is larger than the elastic limit ($\approx$ 25%) that has been documented in the experiment [11] with micron-sized pristine graphene membrane. Also, there is the plastic deformation stage where the stress-strain curve is serrated (Fig. 7). In doing so, each drop at the stress-strain curve is related to a non-elastic event - either flip or irreversible debonding of a C-C interatomic bond - in HDR under tension. The plastic deformation stage

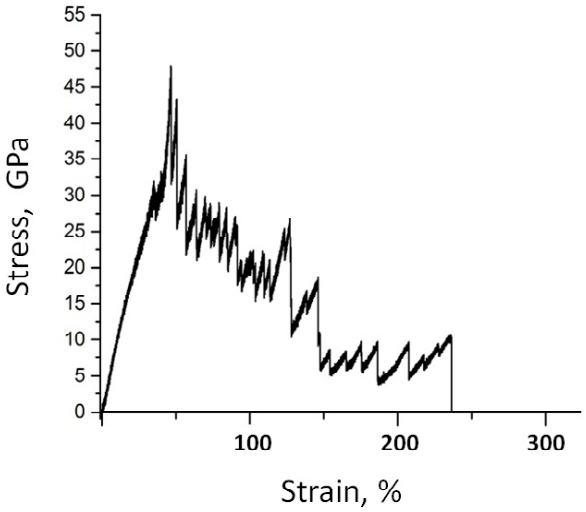

Fig. 7. Stress-strain dependence.

is extended very much (when strain ranges from ≈ 40 to ≈ 234%) and thus indicates on superplasticity of HDG. (It is dramatically contrasted to brittle behaviour typically exhibited by pristine and other graphene structures.) At the same time, the strength of HDG has value (≈ 50 GPa; see Fig. 7) being much lower than the experimentally measured [11] strength (≈ 130 GPa) of pristine graphene membrane.

Note that the plastic deformation stage is logically divided into 2D and 1D deformation sub-stages. HDG as a 2D material is plastically deformed during the former stage occurring from $\varepsilon \approx 40$ to ≈ 148%. Then, nanoscale cracks/pores separate HDG into two pieces joined by a monatomic carbon chain (Fig. 5), and 1D deformation stage occurs which is realized through elongation of the carbon chain. The crossover from 2D to 1D deformation regimes comes into play at $\varepsilon \approx 148\%$. 1D plastic deformation progresses until complete fracture of HDG - complete separation of HDG into two separate pieces (Fig. 6) – at strain-to-failure ≈ 234%.

5. CONCLUDING REMARKS

To summarize, with MD simulations, we have examined deformation and fracture processes in HDG under tensile load. HDG has the nanoscopically curved structure due to 5- and 7-discinations distributed with a high density in this graphene system (Figs. 1 and 2). It is found that HDG exhibits the specific behavioral features owing to disclination-induced curvature. In particular, our simulations revealed that HDG shows superplasticity specified by strain-to-failure ≈ 234% (Fig. 7). The key reason of superplasticity is in the presence of pre-existent disclinations that enhance generation of new disclination dipoles and other disclination configurations effectively carrying plastic flow in graphene (Figs. 3 and 4).

Also, from the stress-strain dependence presented in Fig. 7 it follows that HDG is characterized by both rather high elastic limit $\varepsilon_{el} \approx 40$ % and tensile strength $\sigma_t \approx 50$ GPa. For comparison, in the experiment [11], pristine graphene membrane of micron-sized diameter shows $\varepsilon_{el} \approx 25\%$ and $\sigma_t \approx 130$ GPa. Thus, our simulations have revealed both enhancement of the elastic limit and degradation of the tensile strength of HDG, as compared to pristine graphene.

The presented results are important for understanding the effects of disclination-produced curvature on the mechanical properties of graphene. In the context discussed, of particular interest is superplasticity exhibited by HDG. This highly plastic behavior is contrasted to typical brittle behavior of most graphene structures. At the same time, giant plasticity has been observed in MD simulations of tensile tests with ultranarrow graphene nanoribbons [28] where free surface effects are highly pronounced. The results presented in this paper and those presented in Ref. [28] are indicative of the intriguing (from both fundamental and applied viewpoints) possibility to dramatically enhance plasticity of graphene through insertion of disclinations into it and use of ultranarrow ribbon geometry, respectively.

ACKNOWLEDGEMENTS

This work was supported by the Russian Science Foundation (Project 14-29-00199). The simulations were performed at Resource Center "Simulation Center of St. Petersburg State University".

REFERENCES

[1] A.H. Castro Neto, F. Guinea, N.M.R. Peres, K.S. Novoselov and A.K. Geim // *Rev. Mod. Phys.* **81** (2009) 109.
[2] A.A. Balandin // *Nature Mater.* **10** (2011) 569.
[3] I.A. Ovid'ko // *Rev. Adv. Mater. Sci.* **30** (2012) 201.
[4] K.S. Novoselov, V.I. Fal'ko, L. Colombo, P.R. Gellert, M.G. Schwab and K. Kim // *Nature* **490** (2012) 192.
[5] I.A. Ovid'ko // *Rev. Adv. Mater. Sci.* **34** (2013) 1.
[6] O.V. Yazyev and Y.P. Chen // *Nature Nanotechnol.* **9** (2014) 755.
[7] I.A. Ovid'ko // *Rev. Adv. Mater. Sci.* **38** (2014) 190.

[8] C. Daniels, A. Horning, A. Phillips, D.V.P. Massote, L. Liang, Z. Bullard, B.G. Sumpter and V. Meunier // *J. Phys.: Condens. Matter* **27** (2015) 373002.
[9] J.-W. Jiang, B.-S. Wang, J.-S. Wang and H.S. Park // *J. Phys.: Condens. Matter* **27** (2015) 083001.
[10] I.A. Ovid'ko and A.V. Orlov // *Rev. Adv. Mater. Sci.* **40** (2015) 249.
[11] C. Lee, X. Wei, J.W. Kysar and J. Hone. // *Science* **321** (2008) 385.
[12] M.A.H. Vozmediano, M.I. Katsnelson and F. Guinea // *Phys. Rep.* **496** (2010) 109.
[13] F. Guinea, M.I. Katsnelson and A.K. Geim // *Nature Phys.* **6** (2010) 30.
[14] N. Levy, S.A. Burke, K.L. Meaker, M. Panlasigui, A. Zettl, F. Guinea, A.H. Castro Neto and M.F. Grommie // *Science* **329** (2010) 544.
[15] J. Zabel, R.R. Nair, A. Ott, T. Georgiou, A.K. Geim, K.S. Novoselov and C. Casiraghi // *Nano Lett.* **12** (2011) 617.
[16] V. Atanasov and A. Saxena // *J. Phys.: Condens. Matter*. **23** (2011) 175301.
[17] S. Gupta and A. Saxena // *J. Appl. Phys.* **109** (2011) 074316.
[18] I.A. Ovid'ko // *Rev. Adv. Mater. Sci.* **34** (2013) 12.
[19] Z. Song, V.I. Artyukhov, J. Wu, B.I. Yakobson and Z. Xu // *ASC Nano* **9** (2013) 401.
[20] A.S. Kochnev, N.F. Morozov, I.A. Ovid'ko and B.N. Semebov // *Doklady Physics.* **61** (2016) 239.
[22] S.J. Stuart, A.B. Tutein and J.A. Harrison // *J. Chem. Phys.* **112** (2000) 6472.
[24] R. Grantab, V.B. Shenoy and R.S. Ruoff // *Science* **330** (2010) 946.
[25] Y. Wei, J. Wu, H. Yin, X. Shi, R. Yang and M. Dresselhaus // *Nature Mater*. **11** (2012) 759.
[26] T.-H. Liu, C.-W. Pao and C.-C. Chang // *Carbon* **50** (2012) 3465.
[27] A.S. Kochnev, I.A. Ovid'ko and B.N. Semenov // *Rev. Adv. Mater. Sci.* **37** (2014) 105.
[28] A.S. Kochnev and I.A. Ovid'ko // *Rev. Adv. Mater. Sci.* **43** (2015) 77.
[29] A.S. Kochnev and I.A. Ovid'ko // *Rev. Adv. Mater. Sci.* **43** (2015) 89.
[30] M. Kleman and F. Friedel // *Rev. Adv. Mater. Sci.* **80** (2008) 61.
[31] A.E. Romanov and A.L. Kolesnikova // *Prog. Mater. Sci*. **54** (2009) 740.
[32] I.A. Ovid'ko // *Science* **295** (2002) 2396.
[33] S.V. Bobylev, N.F. Morozov and I.A. Ovid'ko // *Phys. Rev. Lett*. **105** (2010) 055504.
[34] I.A. Ovid'ko and A.G. Sheinerman // *Rev. Adv. Mater. Sci.* **39** (2014) 54.
[35] I.A. Ovid'ko, N.V. Skiba and A.G. Sheinerman // *Rev. Adv. Mater. Sci.* **43** (2015) 38.
[36] F. Ding, K. Jiao, M. Wu and B.I. Yakobson // *Phys. Rev. Lett.* **98** (2007) 075503.
[37] J.H. Warner, E.R. Margine, M. Mukai, A.W. Robertson, F. Giustino and A.I. Kirkland // *Science* **337** (2012) 209.